

Structural analysis of the Cu(100)- $p(3\sqrt{2} \times \sqrt{2})R45^\circ$ -Sn surface using low and medium energy ion scattering spectroscopies

M. Walker^{a,*}, M.G. Brown^a, M. Draxler^a, M.G. Dowsett^a, C.F. McConville^a, T.C.Q. Noakes^b, P. Bailey^b

^a Department of Physics, University of Warwick, Coventry, CV4 7AL, UK

^b STFC Daresbury Laboratory, Daresbury, Warrington, WA4 4AD, UK

ARTICLE INFO

Article history:

Received 23 May 2011

Accepted 7 July 2011

Available online 23 July 2011

Keywords:

Low energy ion scattering (LEIS)
Medium energy ion scattering (MEIS)
Low energy electron diffraction (LEED)
Copper
Tin
Metallic surfaces
Alloys

ABSTRACT

The atomic structure of the Cu(100)- $p(3\sqrt{2} \times \sqrt{2})R45^\circ$ -Sn surface has been studied using medium energy ion scattering (MEIS), co-axial impact collision ion scattering spectroscopy (CAICISS), low energy electron diffraction (LEED) and Auger electron spectroscopy (AES). The $p(3\sqrt{2} \times \sqrt{2})R45^\circ$ reconstruction was observed with LEED following the deposition of 0.42 ML of Sn from a Knudsen cell on to the clean Cu(100) surface. The existence of sub-surface Sn atoms was immediately ruled out by the lack of blocking dips in the MEIS Sn scattered yield. Previously reported Sn overlayer and Cu–Sn surface layer alloy models were tested against the medium and low energy ion scattering data, with the best fit realised following structural optimization of the surface alloy model proposed by Pussi [K. Pussi et al., Surf. Sci. 549 (2004) 24]. Different out-of-plane shifts were observed for Sn atoms depending on their proximity to the missing Cu row.

© 2011 Elsevier B.V. All rights reserved.

1. Introduction

The structural, chemical and electronic characteristics of bi-metallic surfaces can be accurately controlled using model systems in which metallic thin films are grown upon single crystal metal surfaces, such that the resulting surface offers different properties compared to the surfaces of fully-alloyed crystals [1,2]. Potential applications include metallic thin film growth [3–6] and catalytic processes [7,8]. Oftentimes complex surface reconstructions are produced by the deposition process [9–14], including in the case of submonolayer quantities of Sn being deposited on to the surface of clean Cu(100) surface. This is, at least in part, due to the large lattice mismatch (~10%) between Cu and Sn atoms [15]. Five different and distinct reconstructions are observed during the deposition of Sn on to the Cu(100) surface [16–21], the first of which, the Cu(100)- $p(2 \times 2)$ -Sn surface, was the subject of a recent investigation in our group [22].

The Cu(100)- $p(3\sqrt{2} \times \sqrt{2})R45^\circ$ -Sn structure (often referred to as the Phase III structure), was first identified by Argile and Rhead [16], who proposed an overlayer structure with all of the Sn atoms in or near four-fold hollow sites. Through examination of low energy electron diffraction (LEED) I–V data they concluded that the surface unit cell of the Cu(100)- $p(3\sqrt{2} \times \sqrt{2})R45^\circ$ -Sn surface must contain three Sn atoms. Incorporating a missing row along the $\langle 100 \rangle$ direction, as shown in Fig. 1(a), provided the necessary periodicity to recreate

the LEED pattern and also correlated well with the 0.50 ML Sn coverage.

A second model for this surface was proposed by McLoughlin et al. [17], still based on a $p(3\sqrt{2} \times \sqrt{2})R45^\circ$ superlattice but without the missing row. Instead, pairs of Sn atoms in the overlayer are “pinched” together, as shown in Fig. 1(b), providing a means of surface stress relief which is required in a system with such a high mismatch in size between its constituents. Through LEED simulations it was found that the amount of “pinching” produced a noticeable change in the diffraction spots, with a 0.2 Å shift per atom providing the best match with the experimental data.

Pussi et al. [18] extended the study of McLoughlin using tensor LEED, arriving at a third potential model. This structure, shown in Fig. 1(c), is based on a $p(3\sqrt{2} \times \sqrt{2})R45^\circ$ surface alloy, analogous to the McLoughlin overlayer model. Strain is relieved in the Pussi alloy model by both lateral relaxations and rumpling of the near-surface atomic layers. STM studies by Lallo [19] and Nara [20] are consistent with the Pussi alloy model, although the images of Nara do not exhibit the missing Cu row in the $\langle 100 \rangle$ direction. Lallo et al. also suggested an alternative model comprising a Sn overlayer with missing rows in the $\langle 100 \rangle$ direction in the underlying Cu layer, shown in Fig. 1(d). Whilst the authors concede that subsurface missing rows are a less commonly accepted means of surface stress relief, the model is still a viable candidate. Two recent STM studies by Martínez-Blanco [23] and Fuhr [24] have indicated the Pussi model to be the correct structure, however ion scattering techniques are ideally placed to resolve the detailed atomic structure of this particular surface. The study of such complex surfaces also provides a clear demonstration of

* Corresponding author.

E-mail addresses: M.Walker@warwick.ac.uk (M. Walker), C.F.McConville@warwick.ac.uk (C.F. McConville).

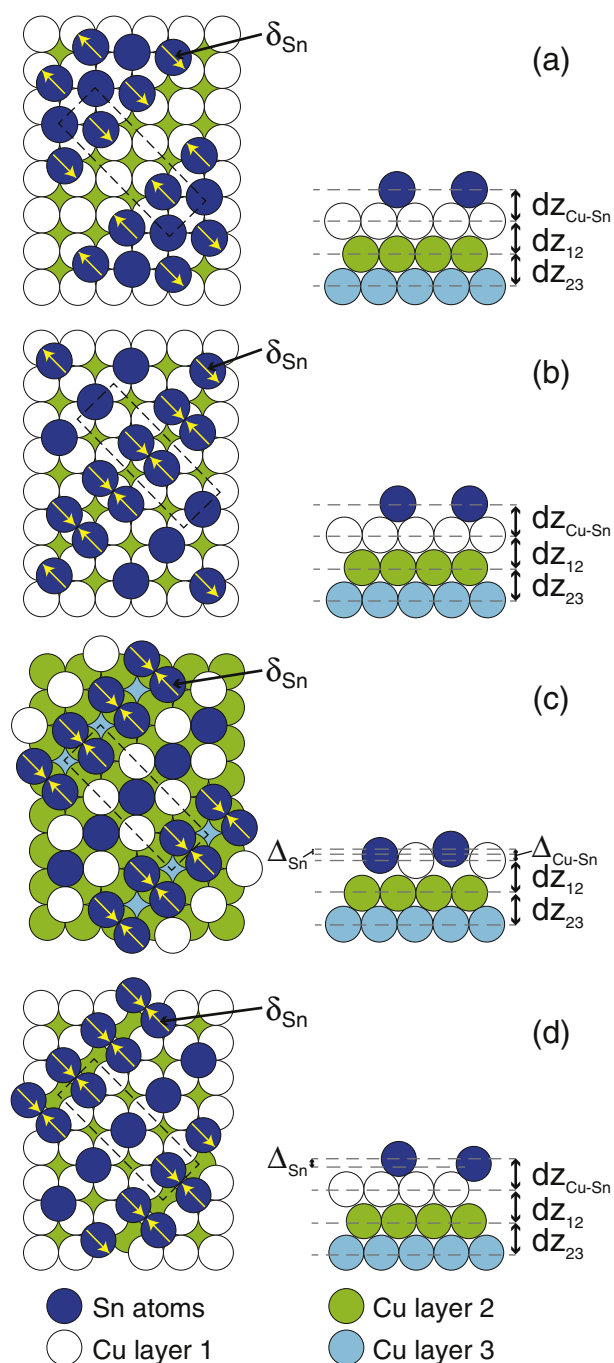


Fig. 1. The four models of the $\text{Cu}(100)-p(3\sqrt{2} \times \sqrt{2})\text{R}45^\circ\text{-Sn}$ surface. (a) The Argile and Rhead model [16]; (b) the McLoughlin model [17]; (c) the Pussi model [18]; (d) the Lallo model [19]. δ_{Sn} denotes the shift of Sn atoms towards the Cu missing row. $\Delta_{\text{Cu-Sn}}$ denotes the out-of-plane shift of Sn atoms relative to the surface layer Cu atoms. dz_{12} and dz_{23} correspond to the first and second interlayer spacings, respectively. In the overlayer models, $dz_{\text{Cu-Sn}}$ corresponds to the distance between the Sn overlayer and the outermost layer of the Cu substrate.

the ability of combining low energy electron diffraction and ion scattering techniques to resolve pressing problems within modern surface science.

2. Experimental and analysis details

In this paper we examine the structure of the $\text{Cu}(100)-p(3\sqrt{2} \times \sqrt{2})\text{R}45^\circ\text{-Sn}$ surface using both co-axial impact collision ion scattering spectroscopy (CAICISS) at the University of Warwick [25,26] and the medium energy ion scattering (MEIS) facility at Daresbury Laboratory

[27,28]. Both systems were equipped with Auger electron spectroscopy (AES) and LEED for the analysis of surface cleanliness and reconstruction, respectively. The finer details of the vacuum systems, surface preparation, data collection and analysis methods were described in our previous work [22]. The $\text{Cu}(100)-p(3\sqrt{2} \times \sqrt{2})\text{R}45^\circ\text{-Sn}$ surface was prepared from the clean $\text{Cu}(100)$ surface using a calibrated Sn deposition rate of $0.012 \pm 0.002 \text{ ML min}^{-1}$, found to be consistent in both chambers. The optimal $p(3\sqrt{2} \times \sqrt{2})\text{R}45^\circ$ LEED pattern was observed at a coverage of $0.42 \pm 0.07 \text{ ML}$. This coverage is slightly lower than those previously reported, possibly indicating that the surface was not completely covered with the ideal structure. However, no signs of patterns reported at lower coverage were observed, whilst increasing the Sn coverage led to a degradation of the LEED pattern.

MEIS data were analysed using the XVEGAS code, whilst the FAN code was employed in the analysis of the CAICISS data. Optimization of the structural models in both cases was performed using an implicit filtering for constrained optimization (IFFCO) routine. Further details of the analysis procedures can be found in our previous work [22].

3. Results and discussion

3.1. LEED and AES

Following cleaning, the $\text{Cu}(100)$ surface exhibited a sharp (1×1) LEED pattern at 74 eV, shown in Fig. 2(a). Subsequently, Sn was deposited on to the surface for 35 min, after which a $p(3\sqrt{2} \times \sqrt{2})\text{R}45^\circ$ pattern was observed at 213 eV, shown in Fig. 2(b). Fig. 2(c) presents a sketch of the pattern, showing some of the diffraction spots more clearly. This pattern is in agreement with previous experimental observations [16–21].

AES data were recorded using a primary electron beam energy of 5 keV, at which the relative sensitivity of the Sn MNN transition is approximately 3.5 times higher than that of the Cu LMM transition [30]. The Auger results, not shown here, exhibited no signs of contamination as a result of the deposition process. The Cu LMM transitions were observed at kinetic energies between 740 eV and 940 eV, with the Sn MNN transitions being observed between 325 eV and 450 eV. Importantly, there was no evidence of O (510 eV) or C (272 eV) in the spectrum. These LEED and AES results allow us to be confident that the application of MEIS and CAICISS to this system will enable an accurate surface structure determination of a well-ordered $\text{Cu}(100)-p(3\sqrt{2} \times \sqrt{2})\text{R}45^\circ\text{-Sn}$ surface, free from any effects due to surface contamination.

3.2. MEIS

The first step in our ion scattering data analysis was to determine whether the deposited Sn atoms had penetrated below the surface of the $\text{Cu}(100)$ structure. If Sn atoms are located below the surface then blocking dips will exist within the Sn scattered yield due to blocking from atoms in the surface layer. As shown in our previous work [22], raw data is collected in sets of two-dimensional tiles, measuring the scattered intensity as functions of both kinetic energy and scattering angle. By projecting these data on to the angular axis, the blocking curves for both Cu and Sn atoms at the surface were extracted (see Fig. 3). The Sn scattered intensity curve clearly shows a complete absence of blocking dips in the $\langle 011 \rangle$ incident geometry. A similar signal was extracted from the $\langle 112 \rangle$ incidence data (not shown). This provides conclusive evidence that the deposited Sn atoms remain in the outermost layer of the $\text{Cu}(100)$ structure with no detectable penetration below the surface. Also shown are the blocking curves arising from ions scattered from Cu atoms in the surface region in both the $\langle 011 \rangle$ and $\langle 112 \rangle$ incidence directions, with the blocking dips numbered in such a way as to correspond with the directions shown in our previous study [22].

Download English Version:

<https://daneshyari.com/en/article/5422755>

Download Persian Version:

<https://daneshyari.com/article/5422755>

[Daneshyari.com](https://daneshyari.com)